Essential Readings in Light Metals: Alumina and Bauxite.
Edited by Don Donaldson and Benny E. Raahauge.

PREDICTION OF HEAT EXCHANGER - HEAT TRANSFER COEFFICIENT DECAY DUE TO FOULING

G. A. O'NEILL

Alumina and Chemicals Division
Alcoa Laboratories
Alcoa Center, Pennsylvania 15069

The reduction over time of the overall heat transfer coefficient in Bayer Process tubular heaters due to DSP fouling is discussed. A mathematical heat transfer model of this problem has been developed. The model is in a general form allowing for the use of different kinetic equations for the DSP formation reaction. Liquor-side heat transfer coefficients are calculated from correlations using the liquor physical properties. Steam-side heat transfer coefficients are calculated using a Nusselt-type equation. The heat transfer model predictions are compared to experimental results.

1.0 INTRODUCTION

A major consideration in Bayer Process modelling is what value to use for the overall heat transfer coefficient (U-factor) of a tubular heater. Another concern is that these U-factors decay over time due to DSP fouling on the liquor side of the heater. The ability to predict these U-factors and their rate of decay is a useful tool for process modelling. Knowledge of the value of the overall heat transfer coefficient for clean and fouled tubes would allow for process simulation under best case and worst case operating conditions.

This paper presents a mathematical heat transfer model that can be used to predict tubular heater U-factors. The model is flexible enough that different rate equations for the desilication reaction can be easily substituted into it. The model also takes into consideration whether the heater tubes are vertical or horizontal because this affects the steam-side heat transfer coefficient. The predicted overall heater transfer coefficients seem to agree well with experimental data.

NOMENCLATURE

A	desilication area; ft^2
a	heat transfer correlation constant; Equation 2.15
A_i	heater tube inner area; ft^2
Al	liquor alumina concentration; g/L
b	heat transfer correlation constant; Equation 2.15
C_{NUS}	constant for Nusselt equation; Equation 2.18
Cp_L	liquor heat capacity; Btu/lb °F
C_s	liquor silica concentration; g/L
$C_{s\infty}$	liquor silica saturation concentration; g/L
DSP	desilication product
f_{si}	weight fraction of silica in DSP
G	mass flux; lb/ft^2 s
g	acceleration of gravity; ft/h^2
h_I	liquor-side heat transfer coefficient; Btu/h ft^2 °F
h_o	steam-side heat transfer coefficient; Btu/h ft^2 °F
k	DSP formation kinetic rate constant; Equation 2.5; L/g min
k_{CND}	condensate thermal conductivity; Btu/h ft °F
k_L	liquor thermal conductivity; Btu/h ft °F
k_m	heater tube thermal conductivity; Btu/h ft °F
k_s	DSP scale thermal conductivity; Btu/h ft °F
L_{NUS}	characteristic length for Nusselt equation; Equation 2.18; ft
$\dot{m}$	liquor mass flow rate; lb/h
N	liquor Na_2O concentration; g/L
Nu	Nusselt number; Equation 2.15
Pr	Prandtl number; Equation 2.15
q	total heat transferred; Btu/h
Re	Reynolds number; Equation 2.15
RES_L	liquor-side resistance; Equation 2.14; h ft^2 °F/Btu

RES_S	DSP scale resistance; Equation 2.6; h ft^2 °F/Btu
RES_{ST}	steam-side resistance; Equation 2.17; h ft^2 °F/Btu
RES_T	heater tube resistance; Equation 2.20; h ft^2 °F/Btu
RES_{TOT}	total heat transfer resistance; Equation 3.2; h ft^2 °F/Btu
r_i	heater tube inner radius; ft
r_o	heater tube outer radius; ft
r_s	heater tube radius with DSP scale; ft
T_{AVG}	average liquor temperature; Equation 3.1; °F
T_F	film temperature; Equation 2.19; °F
T_{IN}	inlet liquor temperature; °F
T_{OUT}	outlet liquor temperature; °F
T_{SAT}	saturation temperature of steam; °F
T_{ST}	steam temperature; °F
T_{WALL}	condensing surface temperature; °F
ΔT_{lm}	log-mean temperature difference; Equation 2.2; °F
U_i	overall heat transfer coefficient based on tube inner area; Btu/h ft^2 °F
U-factor	overall heat transfer coefficient (U_i); Btu/h ft^2 °F
$\dot{V}$	volume flow; ft^3/min

GREEK SYMBOLS

λ	heat of vaporization of water; Btu/lb
μ_{CND}	condensate viscosity; lb/h ft
μ_L	liquor viscosity; lb/h ft
ρ_{CND}	condensate density; lb/ft^3
ρ_s	DSP scale density; g/L
τ	liquor residence time in heater; min

2.0 HEAT TRANSFER MODEL

2.1 Overall Heat Transfer Coefficient

Figure 2.1 is a diagram of a heater tube with scale on its inner surface. The total amount of heat transferred across the tube is given by Equation 2.1.

$$q = U_i \, A_i \, \Delta T_{lm} \qquad (2.1)$$

In Equation 2.1 both U_i and A_i are based on the inside surface area of the tube and ΔT_{lm} is the log-mean temperature difference. For steam condensing on the outside of the tube, the equation for log-mean temperature difference becomes:

$$\Delta T_{lm} = \frac{T_{OUT} - T_{IN}}{\ln\left[\frac{T_{ST} - T_{IN}}{T_{ST} - T_{OUT}}\right]} \qquad (2.2)$$

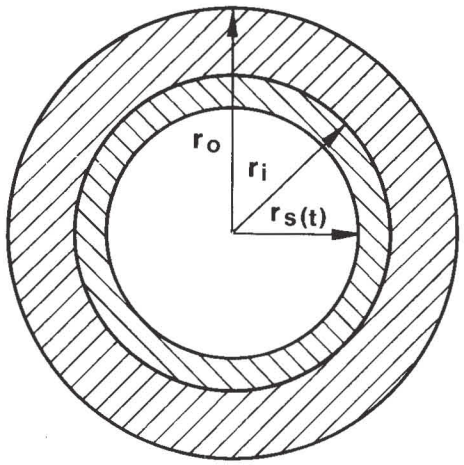

Diagram of Scaled Heater Tube
Figure 2.1

There are four resistances to heat transfer across a fouled heater tube: liquor-side resistance, resistance in the tube scale, resistance across the tube wall, and steam-side resistance. Based on the tube inner area, the overall heat transfer coefficient is related to these four resistances as follows:

$$U_i = \frac{1}{\frac{r_i}{h_i \, r_s(t)} + \frac{r_i \ln\left(\frac{r_i}{r_s(t)}\right)}{k_s} + \frac{r_i \ln\left(\frac{r_o}{r_i}\right)}{k_m} + \frac{r_i}{r_o \, h_o}} \qquad (2.3)$$

In Equation 2.3, $r_s(t)$ is the radius of the tube to the scale which is a function of time as the tube fouls (see Figure 2.1).

2.2 Calculation of Heat Transfer Resistances

2.2.1 DSP Scale Resistance. The resistance to heat transfer of the DSP scale changes over time as the scale thickness increases. The rate of change of scale thickness is governed by the kinetics of

the desilication reaction. Oku and Yamada [1] and Yamada et al. [2] report the desilication rate to be second order with respect to silica supersaturation and give the silica saturation concentration as:

$$C_{s\infty} = 2.7 \times 10^{-5} \cdot N \cdot Al \qquad (2.4)$$

For the current study, the following desilication rate equation was used:

$$\frac{dC_s}{dt} = -k\ (C_s - C_{s\infty})^2 \qquad (2.5)$$

with $k = 244341 \exp(-6166.4/T)$

$T = °K$

The resistance to heat transfer due to the DSP scale is determined by scale thickness which is function of time:

$$RES_S = \frac{r_i \ln\left(\frac{r_i}{r_{s(t)}}\right)}{k_s} \qquad (2.6)$$

To calculate scale thickness as a function of time, Equation 2.5 is used with the following relationship:

$$\frac{dr_s}{dt} = \left(\frac{dC_s}{dt}\right)\left(\frac{dr_s}{dC_s}\right) \qquad (2.7)$$

The second term of Equation 2.7; (dr_s/dC_s); represents the change of scaled tube radius as desilication occurs.

$$\frac{dr_s}{dC_s} = \frac{\dot{V}\tau}{f_{si}\,\rho_s\,A} \qquad (2.8)$$

Substituting Equations 2.5 and 2.8 into Equation 2.7 yields:

$$\frac{dr_s}{dt} = -k\ (C_s - C_{s\infty})^2 \left(\frac{\dot{V}\tau}{f_{si}\,\rho_s\,A}\right) \qquad (2.9)$$

Substituting:

$$\tau = \pi r_s^2 L/\dot{V}$$

$$A = 2\pi r_s L$$

$$\frac{dr_s}{dt} = -k\ (C_s - C_{s\infty})^2 \left(\frac{r_s}{2\,f_{si}\,\rho_s}\right) \qquad (2.10)$$

Integrating Equation 2.10:

$$\int_{r_{old}}^{r_{new}} \frac{dr_s}{r_s} = \frac{-k\ (C_s - C_{s\infty})}{2\,f_{si}\,\rho_s} \int_{t_{old}}^{t_{new}} dt \qquad (2.11)$$

Solving the integral:

$$\ln\left(\frac{r_{new}}{r_{old}}\right) = \frac{-k\ (C_s - C_{s\infty})^2\ (t_{new} - t_{old})}{2\,f_{si}\ s} \qquad (2.12)$$

$$r_{new} = r_{old} \exp\left(\frac{-k\ (C_s - C_{s\infty})\ (t_{new} - t_{old})}{2\,f_{si}\,\rho_s}\right) \qquad (2.13)$$

Substituting Equation 2.13 into Equation 2.6 yields the scale resistance at the end of the time interval $(t_{new} - t_{old})$.

Examining Equation 2.13 reveals that the right side of the desilication rate equation (Equation 2.5) appears in the exponential unchanged. Thus, to use the model with different desilication kinetics, the $-k\ (C_s - C_{s\infty})^2$ term in the exponential of Equation 2.13 is merely replaced with the other kinetic rate equation.

2.2.2 Liquor-Side Resistance. The liquor-side resistance to heat transfer is given by Equation 2.14:

$$RES_L = \frac{r_i}{h_i\ r_s(t)} \qquad (2.14)$$

In Equation 2.14, r_i is a constant and $r_s(t)$ can be solved for using Equation 2.13, thus, only the liquor-side heat transfer coefficient; h_i; must be calculated. Kays and Crawford [3] give a heat transfer correlation for tube flow with liquids having Prandtl numbers greater than 1.0.

$$Nu = \frac{2\ r_s(t)\ h_i}{k_L} = 5 + 0.015\ Re^a\ Pr^b \qquad (2.15)$$

where $a = 0.88 - 0.24/(4 + Pr)$

$b = 0.333 + 0.5 \exp(-0.6\ Pr)$

and $Pr = \frac{\mu_L\ C_{PL}}{k_L}$; $0.1 < Pr < 10^4$

$$Re = \frac{2\ r_s(t)\ G}{\mu_L} \ ; \ 10^4 < Re < 10^6$$

Solving Equation 2.15 for the liquor-side heat transfer coefficient yields:

$$h_i = [5 + 0.015\ Re^a\ Pr^b]\ [k_L/2r_s(t)] \qquad (2.16)$$

Substituting Equation 2.16 into Equation 2.14 gives the liquor-side heat transfer resistance which is used in the calculation of the overall heat transfer resistance.

2.2.3 Steam-Side Resistance. Steam-side resistance to heat transfer is given by Equation 2.17:

$$RES_{ST} = \frac{r_i}{r_o h_o} \qquad (2.17)$$

In Equation 2.17, both r_i and r_o are constant, thus, only the steam-side heat transfer coefficient; h_o; must be calculated. Condensing steam-side heat transfer coefficients can be estimated using a Nusselt-type analysis. The value of h_o is strongly affected by whether the heater tubes are vertical or horizontal. Kern [4] gives the Nusselt equation for both vertical and horizontal tubes. The two equations can be combined into one as follows:

$$h_o = C_{NUS} \left[\frac{k_{CND}^3 \; \rho_{CND}^2 \; \lambda g}{L_{NUS} \; \mu_{CND} \; (T_{SAT} - T_{WALL})} \right]^{1/4} \qquad (2.18)$$

where C_{NUS} = 0.943 for vertical tubes

= 0.725 for horizontal tubes

L_{NUS} = tube length for vertical tubes

= tube diameter for horizontal tubes

All condensate physical properties used in Equation 2.18 are evaluated at the film temperature which is:

$$T_F = 0.5 \; (T_{WALL} + T_{SAT}) \qquad (2.19)$$

In the current study, the steam is assumed to be saturated when calculating h_o, thus, Equation 2.18 is not exact for a system with superheated steam. McAdams [5] states that the rate of heat transfer for superheated steam is only slightly different than that of saturated steam, thus, T_{SAT} can be used in Equation 2.18. The fact that the superheated steam has a slightly higher heat content than saturated steam is offset by the fact that the superheated steam will have a slightly lower condensing heat transfer coefficient than predicted by Equation 2.18.

The steam-side resistance to heat transfer is calculated by substituting h_o, calculated by Equation 2.18, into Equation 2.17.

2.2.4 Tube Resistance. The resistance to heat transfer caused by the tube is calculated as follows:

$$RES_T = \frac{r_i \ln \left(\frac{r_o}{r_i}\right)}{k_m} \qquad (2.20)$$

To calculate tube resistance, r_i and r_o in Equation 2.20 are constants. In addition, k_m is essentially constant over the typical temperature range of a Bayer plant and is considered to be constant by the model.

3.0 SOLVING THE HEAT TRANSFER MODEL

The overall heat transfer coefficient cannot be solved for directly. Because the liquor and condensate physical properties are functions of temperature, the calculation of liquor outlet temperature and overall heat transfer coefficient is iterative.

A completely rigorous solution of the problem would require integration of the equations over the entire length of the tube. This would result in each part of the tube having a different desilication rate dependent upon the local liquor temperature. The result of this would be a tube scale that varied over the length of the tube.

In order to simplify the solution of the heat transfer model, the calculations for desilication rate are made assuming that all the liquor inside the tube is at the average liquor temperature:

$$T_{AVG} = 0.5 \; (T_{IN} + T_{OUT}) \qquad (3.1)$$

The first step in solving the problem is to choose the time interval at which the value of the overall heat transfer coefficient is desired. If the heat transfer coefficient is desired ten days after tube cleaning, the model could be solved once with ten days being set as the time interval. However, a better answer would be obtained by solving the model ten times at one day intervals while updating the old scale thickness input to the model after each time that the model was solved. This method of solving the model ten times would be more accurate because, by updating the scale thickness each day, the outlet tube temperature would change each day which would, in turn, affect the desilication rate. The more small time intervals that the desired time interval is broken into, the more accurate the final answer will be because these individual discrete solutions will more closely approach the smooth, continuous solution.

Once the time interval for solution of the model has been chosen, the silica saturation concentration for the liquor is calculated using Equation 2.4. Next, an estimate of the outlet liquor temperature is made to begin the iterative calculation of the overall heat transfer coefficient. Using the average liquor temperature, the value of k for the desilication kinetics is calculated from Equation 2.5 and new scale thickness is calculated using Equation 2.13. In Equation 2.13, $(t_{new} - t_{old})$ is set to the chosen time interval and r_{old} is set to the scaled tube radius at the beginning of the time interval (t_{old}). If the time interval began with a freshly cleaned tube, r_{old} is set equal to r_i.

The liquor-side heat transfer coefficient is now calculated using Equation 2.16. The average liquor temperature is used to calculate the liquor physical properties. The previously calculated value of r_{new} is used as $r_s(t)$ in calculating the Reynolds number.

The calculation of the steam-side heat transfer coefficient is also an iterative process be-

cause the value of h_o depends on the condensing surface temperature which cannot be calculated until h_o is known. To begin the calculation, an estimate of h_o is made. This is converted into a steam-side resistance using Equation 2.17. All other heat transfer resistances are calculated using Equations 2.6, 2.14, and 2.20. The condensing surface temperature is then calculated by using the fact that the fraction of the overall temperature drop occurring on the steam-side is equal to the ratio of the steam side resistance to the total resistance.

$$RES_{TOT} = RES_{ST} + RES_T + RES_S + RES_L \qquad (3.2)$$

$$T_{WALL} = T_{SAT} - ((T_{SAT} - T_{AVG}) (\frac{RES_{ST}}{RES_{TOT}})) \qquad (3.3)$$

Using this calculated condensing surface temperature, h_o is solved for using Equation 2.18. If the calculated value of h_o equals the value that was estimated, then the estimate for h_o is correct and that value will be used in subsequent calculations. If the values are not equal, a new estimate for h_o is made, T_{wall} and h_o are recalculated, and the iterative process continues until the calculation of h_o converges.

Once all of the resistances have been solved for, U_i can be calculated using Equation 2.3 which is equivalent to:

$$U_i = \frac{1}{RES_{TOT}} \qquad (3.4)$$

Two different calculations of the heat transfer rate can now be made. Solving Equation 2.1 gives the heat transfer rate based on log-mean temperature difference. The heat picked up by the liquor stream is calculated by Equation 3.5:

$$q = \dot{m} Cp_L (T_{OUT} - T_{IN}) \qquad (3.5)$$

If the two calculated values of q are equal, then the estimated liquor outlet temperature is correct and the value of U_i calculated by Equation 3.4 is also correct. If the two calculated values of q are not equal, then a new estimate for T_{OUT} is made and the iterative solution method for U_i continues. A flowsheet outlining this solution algorithm is shown in Figure 3.1.

4.0 PRESENTATION OF RESULTS

The heat transfer model presented here was put into a computer program so that it could be solved quickly and accurately. The computer program was written so that it is completely compatible with the ASPEN Bayer Process simulator in use at Alcoa. By making it compatible with ASPEN, the model has access to the latest liquor physical property data available within Alcoa. In addition, because the ASPEN physical property system is enthalpy based, the additional available heat in superheated steam is accounted for when the simulator condenses the steam. Therefore, even though the steam-side heat transfer coefficient is calculated using the saturation temperature of the steam in Equation 2.18, the additional available heat in superheated steam is accounted for in the overall heat balance.

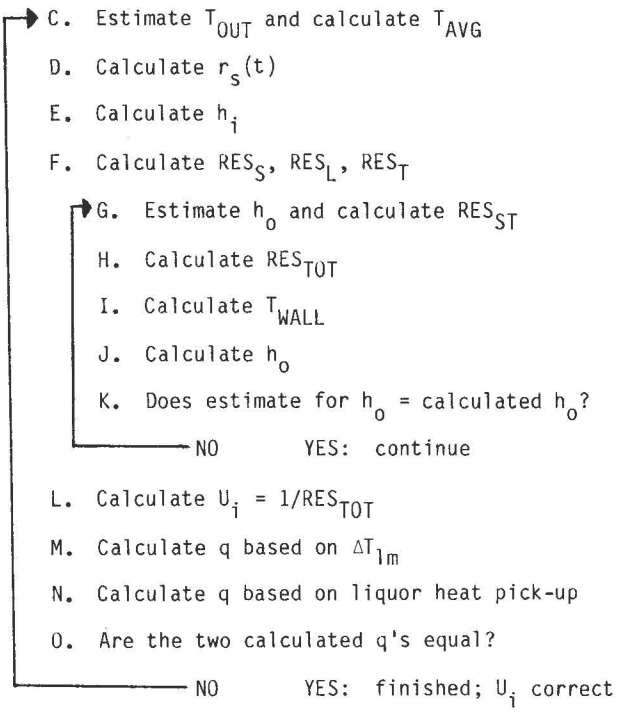

Figure 3.1 Solution Algorithm

Geppert [6] conducted a controlled study on the effect of DSP fouling on the overall heat transfer coefficient of heater tubes. The Geppert study used a four-pass horizontal tube heater assembly in a steam jacket which was held at a constant 306°F. The study lasted 14 days and three different silica levels were used over the course of the test. The four-pass set-up produced results over a large range of liquor temperatures. Geppert used 0.375-inch outer diameter tubes which are smaller than tubes typically used in a Bayer plant. This resulted in the observed U-factors being higher than those usually seen in a plant environment. Unfortunately, Geppert reported heater tube inlet temperatures that were average values over the life of the test. Not having the heater tube inlet temperatures for each day of the test causes some error in the model predictions of overall heat transfer coefficient.

To simulate the 14-day Geppert test, the heat transfer model was solved 15 times. The first run of the model was at time zero to predict the initial U-factor. The next 14 points were spaced at one-day intervals to simulate the remainder of the test. The data plots of the model predictions contained here have fairly sharp changes at Day 2 and Day 6. These were caused by the changes in silica level at those times which caused abrupt changes in the desilication rate.

Figure 4.1 is a comparison between the model predictions and Geppert's experimental data for

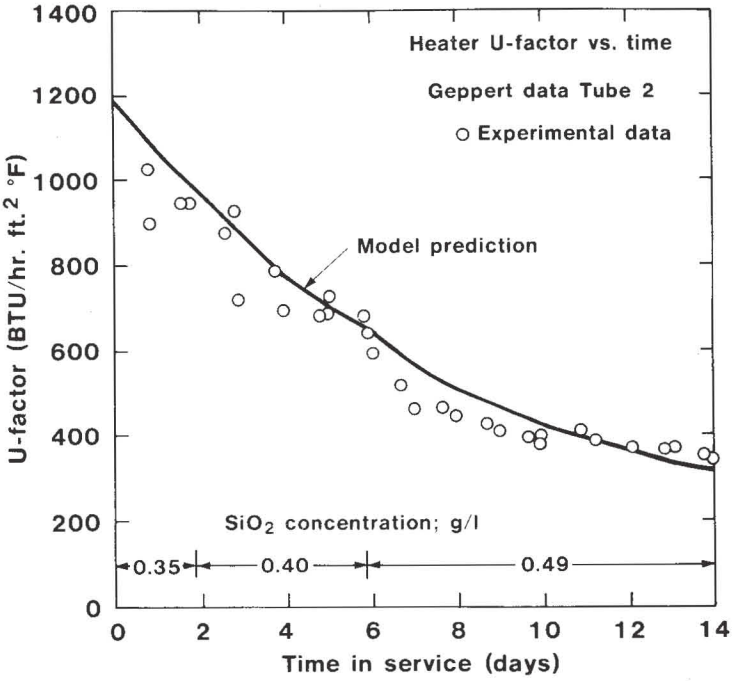

Comparison of Experimental Results and Model Predictions
Figure 4.1

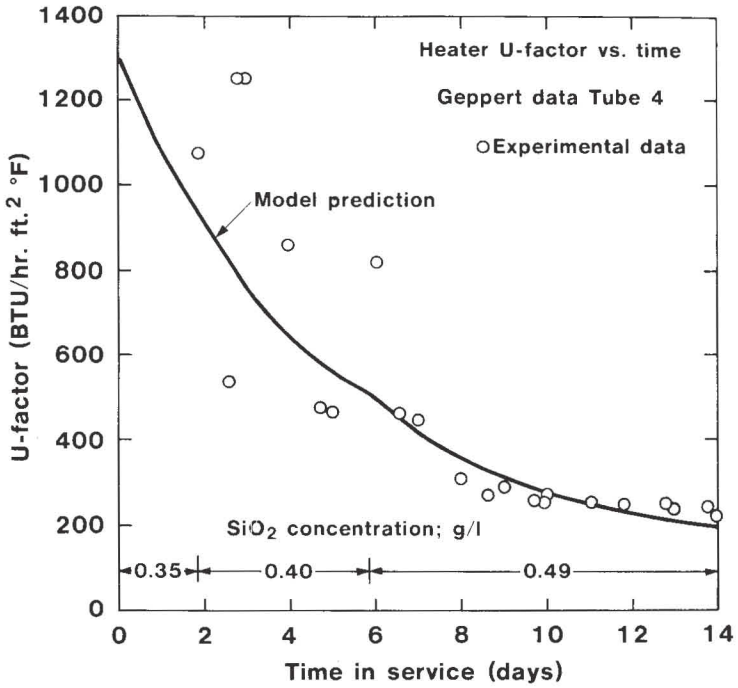

Comparison of Experimental Results and Model Predictions
Figure 4.2

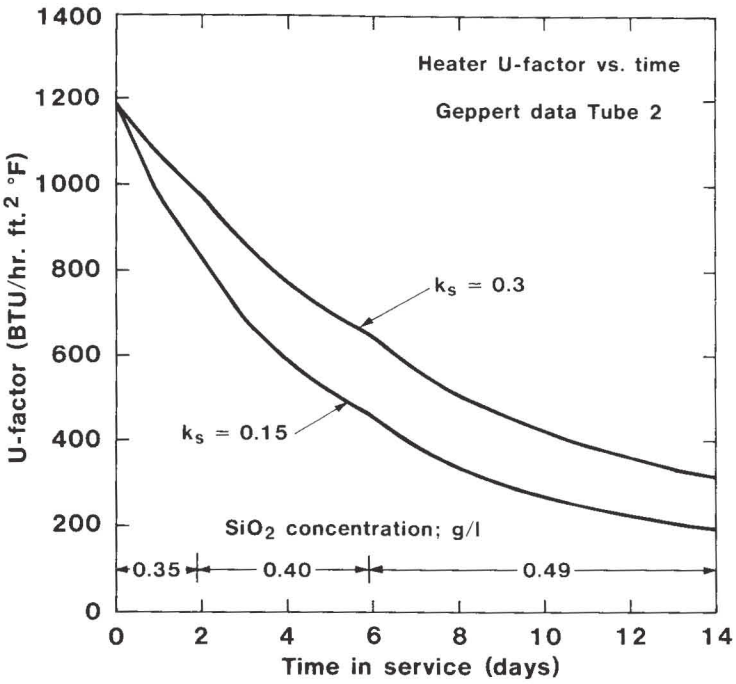

Model Sensitivity to Scale Thermal Conductivity
Figure 4.3

Tube 2. This tube had an average liquor inlet temperature of 241°F. In general, the model predictions are quite close to the slightly scattered data points. Between Days 6 and 10 the predictions are consistently higher than the experimental data. This occurred after the second step increase in the silica concentration which may have contributed to the discrepancy. However, the overall agreement between the model predictions and experimental data is quite good.

Figure 4.2 compares the model predictions to the experimental data for Tube 4 which had an average inlet liquor temperature of 282°F. There is much more scatter in the early data for this tube than for Tube 2. However, where the experimental data are not very scattered, the model predictions are in close agreement with the data.

Comparing the model predictions for these two tubes reveals that the hotter tube (Tube 4) has a higher initial U-factor. However, the U-factor for this tube drops quickly and ends up being much lower than the U-factor for Tube 2. These trends are expected. The hotter tube should start out with a higher U-factor because the $(T_{SAT} - T_{WALL})$ term in the denominator of the equation for steam-side heat transfer coefficient (Equation 2.18) would be smaller. However, the fact that the hotter liquor will desilicate much faster causes the U-factor for Tube 4 to drop more quickly than the U-factor for Tube 2. Thus, the fact that the model predicts a crossing of these U-factor values is easily explained.

The value used for the thermal conductivity of the DSP scale is critical to the accuracy of the model predictions. The thermal conductivity of the scale is so low that it soon becomes the major resistance to heat transfer. The model predictions for Tubes 2 and 4 were made using a value for k_s of 0.3 Btu/h ft °F. Figure 4.3 shows the sensitivity of the heat transfer model to changing in the value of k_s to 0.15 Btu/h ft °F for Tube 2 data. The initial U-factors are the same since there is no scale at time zero. However, within only four days the U-factor for the run with k_s = 0.15 is approximately 200 Btu/h ft² °F lower than the U-factor with k_s = 0.3. As time goes on the U-factors will get closer together because the liquor for the run with k_s = 0.15 will not be as hot and its desilication rate will slow. Figure 4.3 shows the importance of the value of k_s to accurately predicting overall heat transfer coefficients for scaled heater tubes.

5.0 CONCLUSIONS

The heat transfer model developed here is able to fairly accurately predict heater U-factors as well as their decay over time. Agreement between the experimental data presented here and the model predictions is generally good. The model correctly predicts that heaters with a lower temperature driving force will have a higher U-factor than heaters with a higher temperature driving force. The model also agrees with experimental data by predicting that higher temperature heaters will have a faster reduction in U-factor due to the increased desilication rate. The value used for the thermal conductivity of the scale is critical to accurately predicting the heater U-factor as well as its rate of decay over time.

The current model needs to be compared to data from a controlled plant test. This would reveal

whether or not the model is valid for tube dimensions and tube geometry typical of a Bayer plant. One possible improvement to the model would be integrating the equations along the entire tube length rather than using average temperatures, physical properties and kinetics in solving the heat transfer problem. The current model is valid only for solid-free liquors. The handling of slurry heating by the model would also be a useful enhancement.

REFERENCES

1. T. Oku and K. Yamada, "The Dissolution Rate of Quartz and the Rate of Desilication in Bayer Liquor," Light Metals (1971), The Metallurgical Society of AIME, New York, 31-45.

2. K. Yamada, M. Yoshihara and S. Tasaka, "Properties of Scale in Bayer Process," Light Metals (1985), The Metallurgical Society of AIME, New York, 223-235.

3. W. M. Kays and M. E. Crawford, Convective Heat and Mass Transfer (New York: McGraw-Hill Book Company, 1980) 245.

4. Donald Q. Kern, Process Heat Transfer (New York: McGraw-Hill Book Company, 1950) 256-263.

5. William H. McAdams, Heat Transmission, 3rd ed. (New York: McGraw-Hill Book Company, 1954) 351.

6. G. A. Geppert, "Fouling of Tubular Heaters in the CRD System," Progress Report, Alcoa Alumina and Chemicals Division, November 1963.